Chemical Insight into the Origin of Red and Blue Photoluminescence Arising from Freestanding Silicon Nanocrystals

Mita Dasog,[†] Zhenyu Yang,[†] Sarah Regli,[†] Tonya M. Atkins,[§] Angelique Faramus,[⊥] Mani P. Singh,[§] Elayaraja Muthuswamy,[§] Susan M. Kauzlarich,[§] Richard D. Tilley,[⊥] and Jonathan G. C. Veinot[†,‡,*]

[†]Department of Chemistry, University of Alberta, Edmonton, Alberta T6G 2G2, Canada, [‡]NRC-National Institute for Nanotechnology, Edmonton, Alberta T6G 2M9, Canada, [§]Department of Chemistry, University of California, One Shields Avenue, Davis, California 95616, United States, and [⊥]School of Chemical and Physical Sciences and the MacDiarmid Institute for Advanced Materials and Nanotechnology, Victoria University of Wellington, Wellington 6012, New Zealand

ABSTRACT Silicon nanocrystals (Si NCs) are attractive functional materials. They are compatible with standard electronics and communications platforms and are biocompatible. Numerous methods have been developed to realize size-controlled Si NC synthesis. While these procedures produce Si NCs that appear identical, their optical responses can differ dramatically. Si NCs prepared using high-temperature methods routinely exhibit photoluminescence agreeing with the effective mass approximation (EMA), while those prepared *via* solution methods exhibit blue emission that is somewhat independent of particle size. Despite many proposals, a definitive explanation for this difference has been elusive for no less than a decade. This apparent dichotomy brings into question our understanding of Si NC properties and potentially limits the scope of their application. The present contribution takes a substantial step forward toward identifying the origin of the blue emission that is not expected based upon EMA predictions. It describes a detailed comparison of Si NCs obtained from three of the most widely cited procedures as well as the conversion of red-emitting Si NCs to blue emitters upon exposure to nitrogen-containing reagents. Analysis of the evidence is consistent with the hypothesis that the presence of trace nitrogen and oxygen even at the parts per million level in Si NCs gives rise to the blue emission.

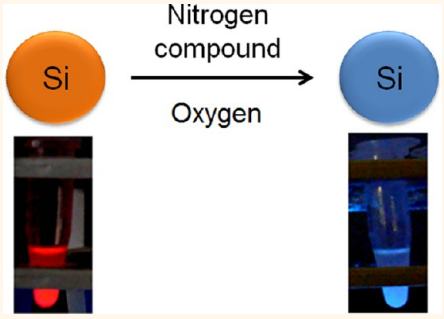

KEYWORDS: silicon nanocrystals · photoluminescence · surface functionalization · nitrogen

The wide-ranging impact of semiconductor nanoparticles, commonly referred to as quantum dots, is well-established.[1,2] Extensive and far-reaching research focused on the synthesis of prototypical Cd-based quantum dots has yielded exquisite control of particle size, shape, and surface chemistry as well as a detailed fundamental understanding of their properties. As a result, there are many prototype applications of these materials in diverse areas, including medical diagnostics, electronics, and solar energy conversion.[3−5] Despite the obvious benefits afforded by the tailorability of Cd-based quantum dots, Cd^{2+} cytotoxicity limits and potentially prevents their widespread use in biological and medical applications. In addition, legislation exists or is pending that could further limit their use in many consumer products.[6] In response, there is a concerted push for "cadmium-free quantum dot" research programs.[7] One approach to addressing these issues is to supplant Cd-based semiconductors with a nontoxic semiconductor. Silicon is a particularly appealing candidate material because it is the second most abundant element in the earth's crust, it is the workhorse material of the electronics industry and its chemistry is well-developed, and, perhaps most importantly, it is biologically benign.

While silicon appears to be the ideal replacement, its indirect band gap and the associated disallowed band gap electronic transition have limited the application of bulk silicon in many photonic applications. When visible light photoluminescence (PL) was observed from porous Si, it brought the promise of linking silicon electronics and photonics.[8] Adding to the appeal are proposals that the optical response of porous Si arose because of the influences of quantum confinement, suggesting that the luminescence should be size-tunable.[9−11] Ever since then, the optical properties of porous and nanocrystalline silicon have been extensively studied and remain the subject of curiosity and even controversy.

* Address correspondence to jveinot@ualberta.ca.

Received for review January 5, 2013 and accepted February 8, 2013.

Published online February 08, 2013
10.1021/nn4000644

Freestanding Si NCs prepared from high-purity reagents at high temperatures or using gas-phase methods exhibit quantum-confined, size-dependent emission analogous to that observed for their CdSe counterparts.[12−15] This quantum-confined band gap emission follows the predictions of the effective mass approximation (EMA) and exhibits long-lived excited state lifetimes (*i.e.*, microseconds)—behavior that is consistent with the bulk Si indirect band gap.[16,17] Unfortunately, this is not the end of the story. There are numerous reports describing visible light emission from Si NCs whose emission maximum is incongruent with the EMA. For example, red-orange PL, frequently identified as the S-band, has been reported for surface-oxidized Si NCs and has been attributed to quasi-direct transitions or surface states.[18−21] Under some circumstances, partially oxidized nanocrystalline silicon shows yellow emission suggested to arise from either surface Si═O species[22] (for which there is currently no known molecular equivalent) or Si−O−C bonds.[23] Of all the visible luminescence arising from Si NCs, the origin of blue PL (frequently termed the F-band) from Si NCs remains one of the most controversial. Most often, this blue PL with fast decay is attributed to a direct band gap transition in ultrasmall Si NCs.[24−30] Alternatively, it has been suggested that the blue PL exhibited by some Si NCs originates from defect states in a surface suboxide, and such luminescence from these NCs does not follow the EMA.[31−34] To our knowledge, no definitive explanation for why certain oxide defects in Si NCs emit orange-red while others emit blue light has been provided. The origin of Si NC emission is clearly complex and involves many contributing factors. If the full potential of Si NCs is to be realized, it is essential that their luminescent properties be understood and effectively controlled.

Generally, Si NCs showing blue PL that does not follow the EMA are prepared using solution methods at comparatively low temperatures (*i.e.*, <400 °C). The reactions leading to the formation of the Si NCs typically involve direct reduction of silicon halides[35−37] or reaction of Zintl salts.[38,39] After careful inspection of the reported conditions employed during these syntheses, we have identified that most employ reagents (*vide infra*) that could supply nitrogen impurities. It is reasonable that nitrogen impurities supplied from these reagents could provide an alternative short-lived excited state that gives rise to the Si NC blue emission.

Herein, we describe a systematic study designed to explore the influence of common nitrogen-containing reagents on the optical behavior of Si NCs with the intent of bringing *chemical* insight to the red *versus* blue debate. We have found that titrating quantum-confined red-emitting Si NCs obtained from the well-established thermolysis of hydrogen silsesquioxane (HSQ) with identified nitrogen sources induces blue PL (Scheme 1). Detailed spectroscopic and electron microscopy characterization of the titrated red-emitting Si NCs and blue-emitting Si NCs obtained from traditional solution-phase methods show trace nitrogen dopants at concentrations near or below detection limits of standard analytical methods. Most importantly, we show definitively that nitrogen and oxygen are present in all Si NCs investigated here that show blue PL. We further demonstrate that emission maximum of the blue emission exhibits solvatochromism, consistent with it originating from a charge transfer state on the NC surfaces.

RESULTS AND DISCUSSION

Hydride Surface-Terminated Si NCs. Oxide-embedded Si NCs were obtained from the thermally induced disproportionation of HSQ, a high-purity electronics grade material containing sub-10 ppb concentrations of metal impurities. This product shows broad reflections in the X-ray powder diffraction (XRD) pattern that are characteristic of nanocrystalline Si adopting the diamond crystal structure (Supporting Information Figure S1A). In addition, a broad reflection arising from the amorphous silica matrix is observed at *ca.* 20°. This Si NC/SiO_2 composite was etched with 1:1:1 49% hydrofluoric acid/ethanol/water to liberate hydride surface-terminated Si NCs (*i.e.*, H−Si NCs). The presence of the Si−H surface was confirmed using FT-IR spectroscopy, which showed characteristic stretching at *ca.* 2100 cm^{-1}. Weak Si−O−Si and Si−OH stretches are also noted at *ca.* $\leq$1200 and $\geq$3000 cm^{-1}, respectively, and result from trace oxidation of the NC surface occurring during sample preparation.[14] The PL spectrum of a toluene solution of H−Si NCs shows a maximum at 630 nm upon excitation at 300 nm. Excited state lifetime measurements provide a lifetime of τ = 1.6 μs, in agreement with previous reports attributing the luminescence to an indirect band gap transition.[17] A bright-field transmission electron microscopy (TEM) image shows 3.5 $\pm$ 0.4 nm average particle diameter consistent with the EMA. It is of significant importance to note that the extreme air sensitivity and limited solubility of H−Si NCs limits the accuracy of direct TEM characterization; however, particle dimensions are consistent with those obtained for dodecyl surface-functionalized (Si NC-A) obtained from post-etching hydrosilylation (*vide infra*). Representative data for the characterization of H−Si NCs are shown in Figure S1A−E.

Dodecyl Surface-Terminated Si NCs Obtained from HSQ (Si NC-A). Alkyl surface functionalization of H−Si NCs is routinely achieved *via* thermally induced hydrosilylation of surface Si−H moieties. This procedure renders Si NCs air-stable for months and compatible with a variety of solvents, thereby making handling and characterization more straightforward. For the present study, surface functionalization of H−Si NCs with dodecyl surface moieties is necessary for direct comparison with alkyl surface-functionalized Si NCs obtained directly from the reaction of sodium silicide and ammonium bromide (*vide infra*). Dodecyl surface-functionalized Si NCs (Si NC-A) were prepared using established literature procedures.[40] The

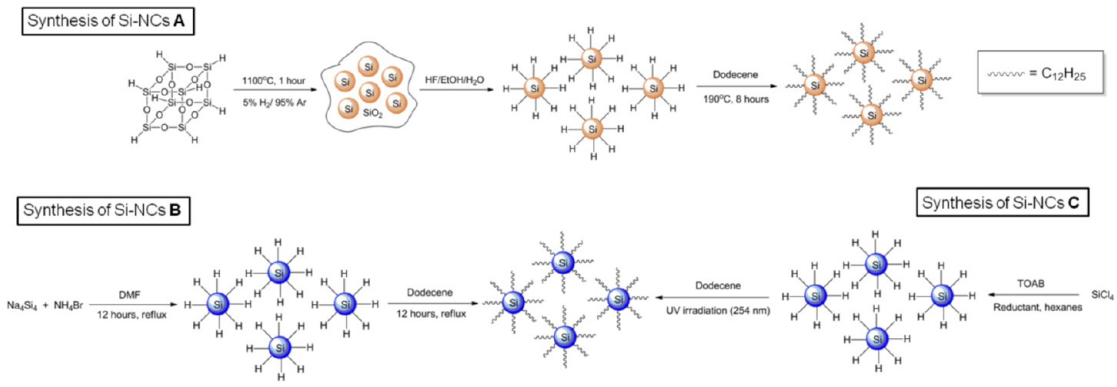

Scheme 1. Schematic representation of the three synthetic approaches used to prepare alkyl-passivated Si nanocrystals (Si NCs) used in this study. (Top) Synthesis of red-emitting H−Si NC and Si NC-A using hydrogen silsesquioxane (HSQ). (Bottom) Synthesis of blue-emitting Si NC-B and Si NC-C.

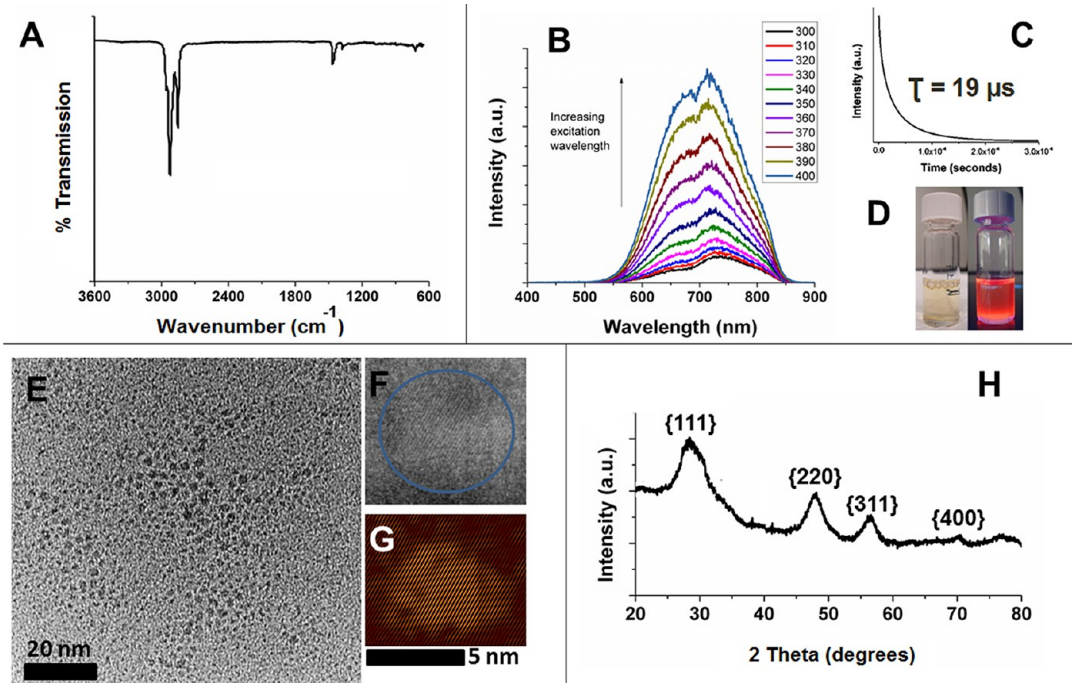

Figure 1. Summary of the characterization of dodecyl-terminated Si NCs (Si NC-A) derived from HSQ. (A) FT-IR spectrum drop-coated from a toluene solution. (B) Photoluminescence (PL) spectra of a toluene solution excited at indicated wavelengths. (C) Photoluminescence decay used to determine excited state lifetimes upon exciting with the 349 nm laser. (D) Toluene dispersions of dodecyl-terminated Si NCs under ambient (left) and UV irradiation (right). (E) Bright-field transmission electron micrograph (TEM) of *ca.* 3.5 ± 0.4 nm diameter NCs. (F) High-resolution transmission electron micrograph showing fringes of 0.33 nm characteristic of the Si{111} lattice spacing. (G) Inverse Fourier transform of the HRTEM image in F (performed using DigitalMicrograph software). (H) X-ray powder diffraction pattern. Reflections have been indexed to those of the Si diamond structure. The particle size was determined to be *ca.* 3 nm by Scherrer analysis.

resulting Si NC-A were evaluated using a variety of techniques. The FT-IR spectrum (Figure 1A) clearly shows the appearance of C−H stretching at *ca.* 2900 cm^{-1} and no evidence of Si−H stretching at 2100 cm^{-1}. As was the case for H−Si NCs, the presence of some trace oxidation is evidenced by the appearance of Si−O−Si stretch at *ca.* 1100 cm^{-1}. The X-ray photoelectron spectroscopy (XPS) of Si NC-A shows emissions arising only from silicon, carbon, and oxygen (Figure S2A). The Si 2p spectral region has components characteristic of Si(0), Si−C, and silicon suboxide species (Figure S2B). The PL spectrum (λ_{ex} = 350 nm) obtained from a non-opalescent toluene solution of Si NCs-A shows an emission maximum at *ca.* 720 nm (Figure 1B). PL lifetime measurements (Figure 1C) provide values in the microsecond regime (*i.e.*, τ = 19 μs), in agreement with emission lifetimes expected from indirect band gap semiconductors.[17] The red PL (Figure 1D) is consistent with an EMA estimate of particles size of 3.3 nm,[41] which is in agreement with TEM (3.5 ± 0.4 nm), high-resolution (HR) TEM, and XRD (3.6 nm) analysis (Figure 1E−H).

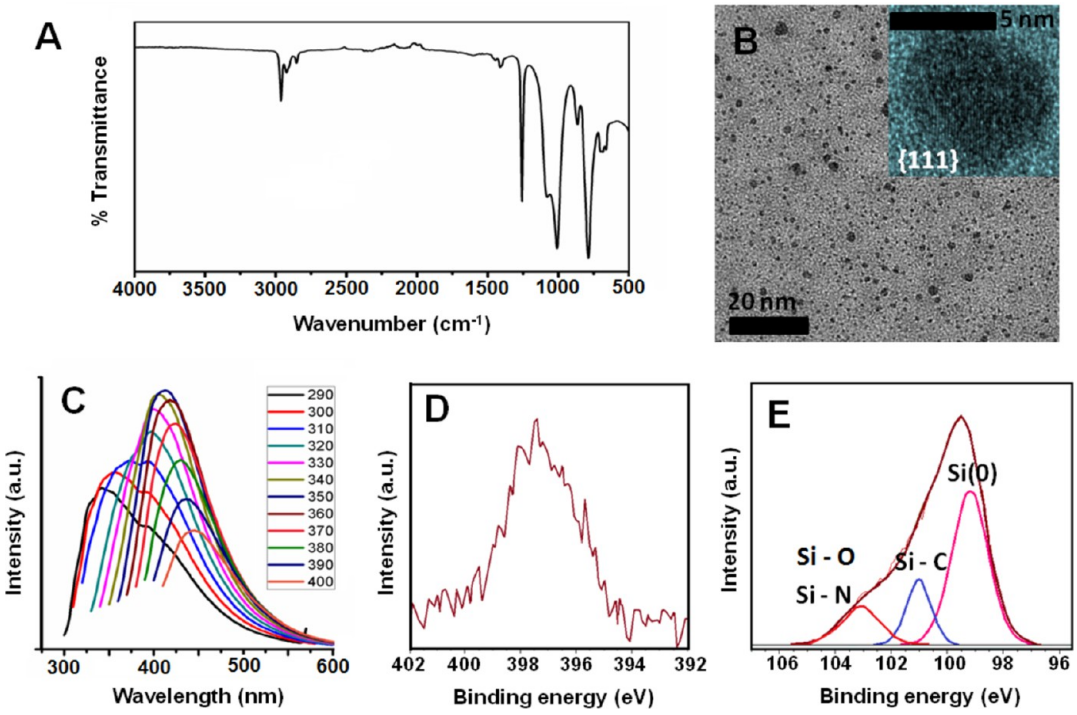

Figure 2. Characterization of dodecyl surface-terminated Si NCs (Si NC-B) obtained from the reaction of Na_4Si_4 with NH_4Br. (A) FT-IR spectrum of Si NCs-B. (B) Bright-field TEM image of *ca.* 6 ± 2 nm diameter NCs. Inset: High-resolution TEM image showing lattice spacings of 0.32 nm characteristic of the {111} plane. (C) Excitation wavelength-dependent PL spectra in toluene. High-resolution X-ray photoelectron spectra (XPS) of the (D) N 1s and (E) Si 2p spectral regions. Experimental (red) and fit (brown) data are provided. Only Si $2p_{2/3}$ fitting peaks are shown. Si $2p_{1/2}$ components have been omitted for clarity.

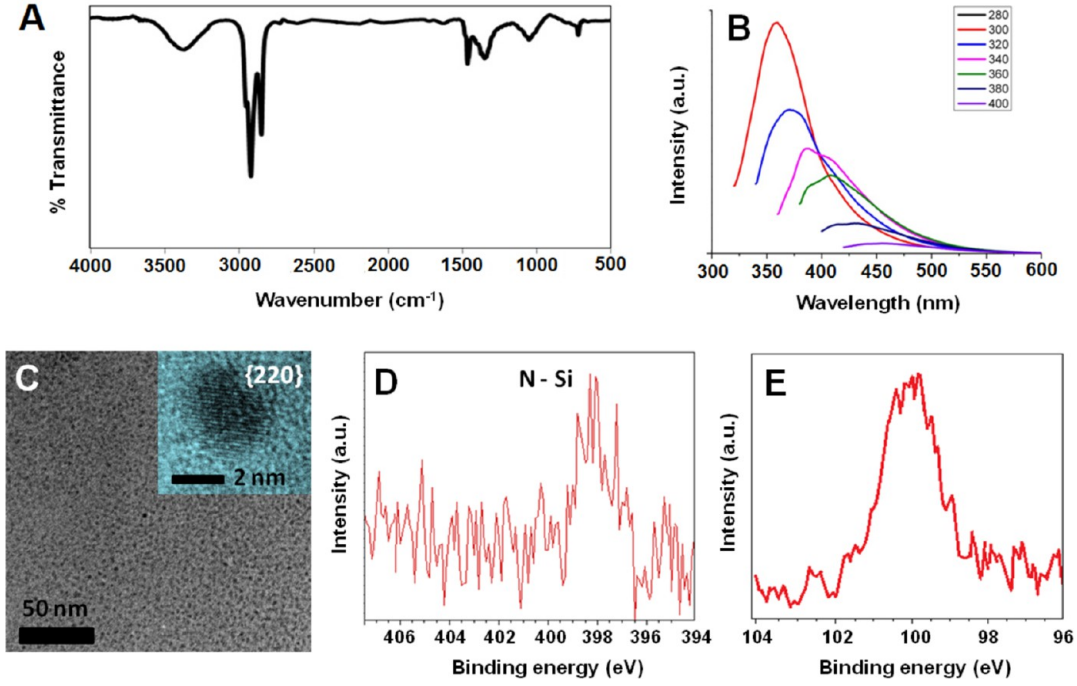

Figure 3. Characterization of dodecyl surface-terminated Si NCs (Si NC-C) obtained from the reduction of $SiCl_4$. (A) FT-IR spectrum of Si NC-C. (B) Excitation wavelength dependence of the PL spectra obtained in toluene. (C) Bright-field TEM micrograph of *ca.* 2.7 ± 0.6 nm diameter Si NC-C. Inset: High-resolution TEM of Si NC-C obtained at 300 kV accelerating voltage showing fringes of 0.192 nm characteristic of the Si{220} lattice spacing. High-resolution XP spectra of the (D) N 1s and (E) Si 2p spectral regions.

Dodecyl Surface-Terminated Si NCs from the Na_4Si_4/NH_4Br Reaction (Si NC-B). Si NCs were obtained by reacting sodium silicide with ammonium bromide salt. The intermediate H–Si NCs are never isolated in this reaction but directly terminated with dodecyl surface groups *via* thermal hydrosilylation (Si NC-B). As is the

case for all Si NCs presented here, the FT-IR spectrum shows expected absorption features (Figure 2A), along with a spectral feature associated with silicon oxide at *ca.* 1100−1030 cm^{-1}. This Zintl salt-based method produces comparatively polydispersed NCs with TEM analysis, indicating a Si core diameter of *ca.* 6 ± 2 nm for Si NC-B (Figure 2B). Si NC-B exhibited an unstructured excitation wavelength-dependent PL spectrum in the blue spectral region that corresponds to an EMA dimension of *ca.* 1.1 nm, which is incongruent with TEM data (Figure 2C). In addition, short nanosecond excited state lifetimes (*i.e.*, τ < 10 ns) inconsistent with a band gap transition have been reported for these Si NCs.[42,43] XPS analysis of Si NC-B shows expected Si, O, and C elemental signatures as well as a low-intensity emission in the N 1s spectral region (Figure 2D,E). The peak at 103.2 eV in the Si 2p spectrum is consistent with a Si−N and Si−O species. The N 1s peak position is consistent with the nitrogen impurities being primarily located on the inside or subsurface of the Si NC.[44]

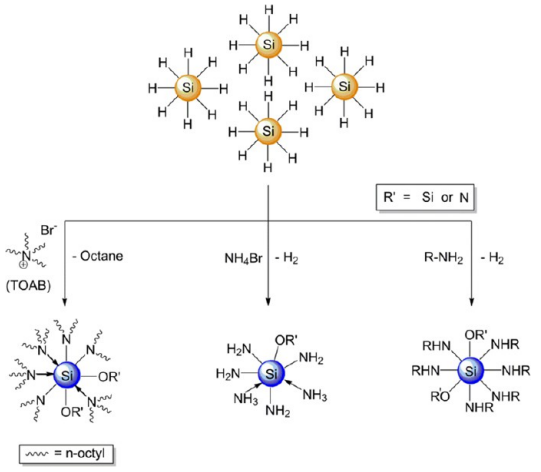

Scheme 2. Schematic representation of the experimental approach to forming blue-emitting Si NCs from exposure of H−Si NCs to common nitrogen sources (RNH_2, NH_4Br, and tetraoctylammonium bromide (TOAB)).

Dodecyl Surface-Terminated Si NCs from $SiCl_4$ Reduction (Si NC-C). H−Si NCs are not isolated from the direct solution reduction of silicon tetrachloride. They are transient reaction species that are functionalized *in situ via* hydrosilylation in the presence of dodecene, and surface-functionalized Si NCs are obtained directly. The FT-IR spectrum of dodecyl (Si NC-C)-terminated Si NCs (Figure 3A) prepared using this procedure shows spectral features arising from the expected functional groups as well as Si−O−Si absorptions. The PL spectra obtained for Si NC-C show excitation wavelength-dependent emission maxima in the blue spectral region (Figure 3B). In addition, much shorter excited state lifetimes (*i.e.*, τ = 4 ns) have been reported, suggesting that a band gap transition is not responsible.[36] TEM/HRTEM analysis indicates Si core dimensions of 2.7 ± 0.6 nm for Si NC-C (Figure 3C). The X-ray photoelectron spectra (XPS) of Si NC-C showed the expected elemental signatures; however, surprisingly, they also showed a

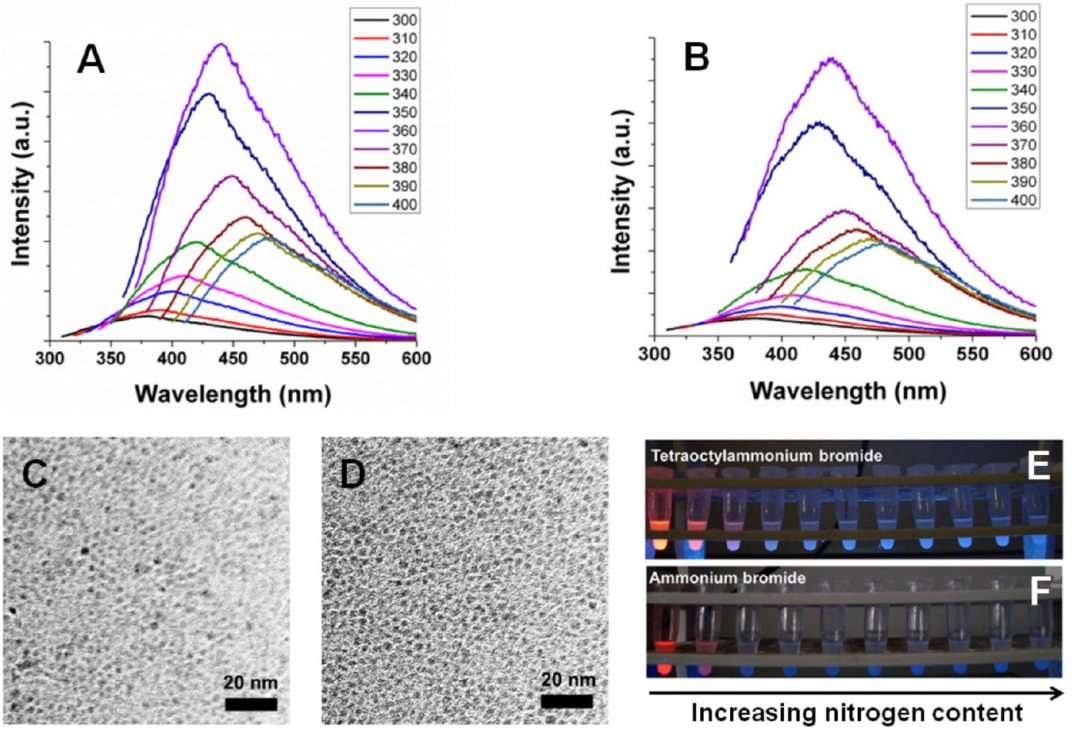

Figure 4. Excitation wavelength-dependent PL of H−Si NCs reacted with (A) TOAB and (B) NH_4Br. TEM images of H−Si NCs reacted with (C) TOAB and (D) NH_4Br. Photograph of H−Si NCs under UV illumination that are reacted with (E) TOAB and (F) NH_4Br.

low-intensity emission in the N 1s spectral region (Figure 3D,E). The higher binding energy of the N 1s spectrum of the Si NC-C compared to that observed for Si NC-B suggests that the N atoms are primarily in the surface of NCs obtained from $SiCl_4$ reduction.[45]

A straightforward comparison of the Si NCs studied here indicates those exhibiting blue emission (*i.e.*, Si NC-B and Si NC-C) contain nitrogen impurities that could give rise to radiative centers that provide an alternative relaxation pathway to an indirect band gap transition. In this context, an experimental demonstration showing that the PL maximum and excited state lifetimes of well-defined Si NCs would add clarity to the broader discussion regarding the origin of blue luminescence and be an invaluable advance in Si NC research and applications. For the blue-emitting Si NCs described here, the experimental nitrogen sources are not necessarily obvious because the nitrogen-containing reagents are frequently used in nanoparticle synthesis and are often considered spectators to the reaction. In this regard, we have systematically evaluated potential nitrogen sources present in the syntheses of Si NC-B and Si NC-C (*i.e.*, tetraoctylammonium bromide (TOAB) and ammonium bromide (NH_4Br)) in efforts to shift the luminescent response of H−Si NCs from EMA consistent red to the characteristic blue emission. To investigate the influence of these nitrogen-containing compounds, we titrated these reagents into solutions of H−Si NCs (Scheme 2).

Influence of TOAB and NH_4Br on H−Si NC Photoluminescence. The Si−H moiety is a very reactive species that may be converted into Si−X (X = C, N, O, S, halide, *etc.*) under relatively mild conditions.[46] TOAB reacts with H−Si NCs to initially form trioctylamine, which is suggested by XPS (N 1s peak at 399.7 eV, Figure S3A).[47] The resulting trioctylamine binds coordinatively to the Si surface (N 1s peak at 398.8 eV, Si $2p_{3/2}$ peak at 100.7 eV, Figure S3B) and undergoes further reduction to yield octane (see ^{1}H NMR, Figure S4) and dioctylamine that bond covalently to the Si surface (N 1s peak at 398.0 eV and Si $2p_{3/2}$ peak at 102.8 eV). Various bonding environments are expected to complicate detailed interpretation of the XPS data; however, a significant quantity of oxygen-containing silicon species is present that is evident from the Si 2p XP spectrum. H−Si NCs reacted with TOAB exhibited excitation wavelength-dependent blue PL (Figure 4A) and short excited state lifetimes (*i.e.*, *ca.* τ = 2.06 ns, Figure S5A). TEM analyses confirm that these changes in PL do not arise from changes in NC size (Figure 4C). The evolution of the blue PL with increasing concentration of TOAB is shown in Figure 4E.

H−Si NCs also react with NH_4Br and change their emission color from red to blue. The excited state lifetime was found to be τ = 1.00 ns (Figure S5B), and excitation wavelength-dependent emission was noted (Figure 4B). Si NC size was found to be 3.8 ± 0.7 nm by TEM (Figure 4D). The relative PL intensity of the Si NCs treated with NH_4Br is lower than that of other blue-emitting Si NCs (Figure 4F). This lower intensity PL could result from the limited solubility of $-NH_2$-functionalized Si NCs in the solvent medium. The formation of a covalent Si−N and Si−O bond is confirmed by XPS (Figure S3C,D). Both in the case of TOAB and NH_4Br, very low concentrations of nitrogen compounds (<0.2 atom % nitrogen) are required to induce blue PL (Figure S6).

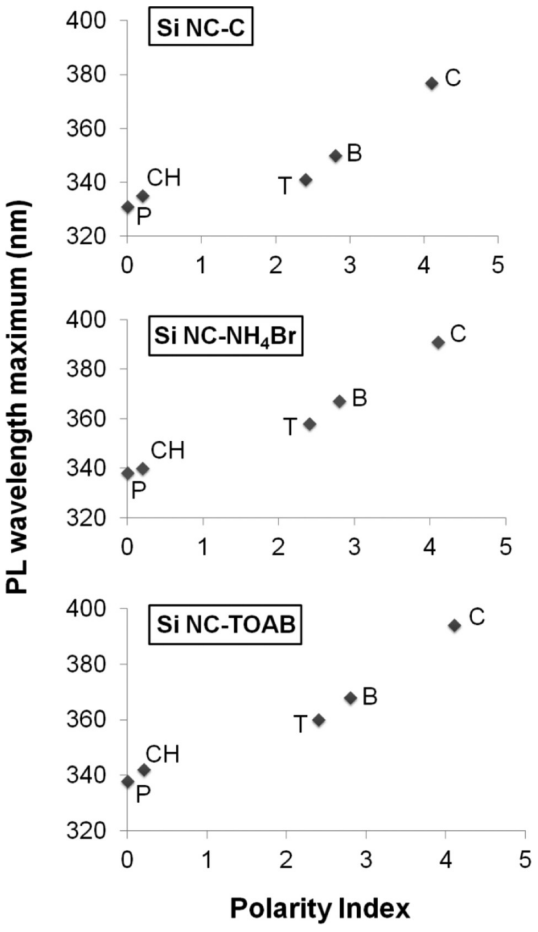

Figure 5. PL maximum *vs* solvent polarity for different Si NCs. P, pentane; CH, cyclohexane; T, toluene; B, benzene; and C, chloroform. The Si NC concentration was 1 mg/mL, and the excitation wavelength was 300 nm.

Control experiments in which H−Si NCs were exposed to TOAB and NH_4Br in the absence of air resulted in no blue PL, and the red luminescence was quenched. Similarly, H−Si NCs were exposed to air in the absence of nitrogen compounds to oxidize the surface, and no blue PL was observed. These observations indicate that both nitrogen and oxygen are crucial for the appearance of blue PL in the present Si NCs.

Solvatochromism Studies. Our observations are consistent with nitrogen and oxygen being necessary to induce blue emission from all of the Si NCs presented here. Blue PL has been reported for SiO_xN_y materials;[48−50] however, the exact mechanism remains unknown. Nekrashevich *et al.* have calculated the electronic structure of silicon

oxynitride and proposed a possible charge transfer from silicon to nitrogen or oxygen centers as its origin.[51] Similarly, Green *et al.* reported blue PL from silicon carboxylate structures that originated from the charge transfer mechanism.[52] Charge-transfer-based PL bands usually lie in the UV−vis region, have short-lived excited states, and exhibit solvatochromic response.[53] To verify the possible role of the charge transfer mechanism in the origin of blue PL in the present systems, we obtained PL spectra in solvents of varied polarity. PL spectra were collected for Si NC-C as well as H−Si NC reacted with TOAB and NH_4Br. In all cases, the PL maximum red-shifted with increasing solvent polarity, consistent with a charge transfer excited state (Figure 5).[53] We observed a shift of ~50 nm in PL emission maximum by changing the solvent from pentane to chloroform. Red luminescent from Si NC-A and blue luminescent Si NC-B did not exhibit solvatochromic response. The lack of Si NC-B solvatochromism response is believed to be the result of the nitrogen impurities being localized within the particle and inaccessible to the solvent medium, consistent with XPS data presented here.

SUMMARY AND CONCLUSIONS

Trace nitrogen and oxygen contamination of the presented Si NC samples was confirmed by XPS analysis and provides a reasonable explanation for the fast blue emission. The present study definitively shows that the Si NCs prepared by two of the low-temperature solution methods contain nitrogen/oxygen and that exposure of H−Si NCs to nitrogen-containing reagents in the presence of oxygen effectively induces blue PL. Both of these findings support the hypothesis that a nitrogen defect or impurity site provides the mechanism of the blue emission. While the exact identity of the nitrogen-containing surface species remains unknown, it is clear that the reactivity of Si−H surfaces must be considered when preparing luminescent Si NCs. Ongoing studies are aimed at identifying the emissive center and exploring methods to tailor its optical response.

METHODS AND MATERIALS

Materials. All reagents were used as received unless noted otherwise. A methyl isobutyl ketone (MIBK) solution of hydrogen silsesquioxane (HSQ) (*i.e.*, FOx 16) was obtained from Dow Corning. Electronic grade hydrofluoric acid (HF, 49%) was purchased from J.T. Baker. 1-Dodecene was purchased from Sigma Aldrich and filtered through activated alumina to remove any peroxide impurities immediately before use. Tetraoctylammonium bromide (TOAB, 98%), allylamine (>99%), reagent grade toluene, chloroform, hydrochloric acid, ethanol, methanol, and acetonitrile were obtained from Sigma Aldrich. Sodium silicide (Na_4Si_4) was purchased from SiGNa Chemistry, Inc. *N*,*N*-Dimethylformamide (DMF) (Sigma-Aldrich, >99%) was degassed and distilled over sodium metal under reduced pressure.

Synthesis of Oxide-Embedded Silicon Nanocrystals (Si NCs). Si NCs embedded within a SiO_2-like matrix were prepared using a well-established literature procedure. In brief, the MIBK was removed from the FOx-16 *in vacuo*, leaving white HSQ powder. The solid was heated to 1100 °C for 1 h under a reducing atmosphere of 5% H_2/95% Ar in a quartz boat within a standard Lindberg Blue tube furnace. After being cooled to room temperature, the resulting dark brown composite made up of Si NCs (diameter *ca.* 4 nm) embedded within a silica (SiO_2) matrix was obtained. This composite was ground to a fine powder using a mortar and pestle and subsequently etched with hydrofluoric acid to liberate hydride surface-terminated Si NCs (*vide infra*).

Preparation of Hydride-Terminated Si NCs. Freestanding hydride-terminated Si NCs were liberated from the oxide matrix *via* hydrofluoric acid etching. Approximately 1 g of Si NC/SiO_2 composite was transferred to a Teflon beaker, and 30 mL of a 1:1:1 mixture of HF/H_2O/C_2H_5OH was added with stirring in subdued light. (Caution: Hydrofluoric acid is extremely dangerous and must be handled with great care.) The resulting dark brown, cloudy mixture was stirred for 1 h. Hydrophobic hydride-terminated Si NCs were extracted from the aqueous etching mixture using three 20 mL toluene extractions. The remaining aqueous solution was colorless and transparent. All remaining HF was neutralized using a saturated solution of calcium chloride. The dark brown Si NC/toluene extracts were placed into glass test tubes and centrifuged using a low-speed centrifuge for 5 min. After centrifugation, the toluene supernatant was decanted, leaving a precipitate of hydride-terminated Si NCs.

Surface Functionalization of Si NCs with Dodecene (Si NC-A). The surfaces of hydride-terminated Si NCs were modified with dodecyl moieties using established literature methods for thermally induced hydrosilylation. Hydride-terminated Si NCs were redispersed in 50 mL of 1-dodecene and transferred into an oven-dried Schlenk flask. The cloudy brown suspension was degassed using three vacuum pump cycles and maintained under a dry argon atmosphere. The flask was placed in a silicone oil bath and heated to 190 °C for 12 h. After reaction, a transparent orange-brown solution was obtained, indicating colloidal stability and consistent with effective functionalization. The reaction mixture was divided equally between four 50 mL PTFE centrifuge tubes. NCs were precipitated using a 3:1 mixture of C_2H_5OH/CH_3OH (20 mL). Particles were centrifuged at 14 000 rpm for 20 min using a Beckman J2-21 high-speed centrifuge, followed by decanting of the supernatant. Three dissolution/precipitation/centrifugation cycles were performed using a chloroform/MeOH solvent/antisolvent pair. After the final precipitation, the functionalized Si NCs were dispersed in toluene, filtered through a hydrophobic PTFE filter, and stored in a sealed vial under argon atmosphere until further use.

Titration of Hydride-Terminated Si NCs with Nitrogen Sources. Freshly prepared hydride-terminated Si NCs (0.32 g) were suspended in toluene (20.00 mL) to yield a 0.50 M solution based upon silicon. Freshly prepared toluene solutions of tetraoctylammonium bromide (0.50 M, 25.00 mL) and ethanol solutions of ammonium bromide (0.50 M, 25.00 mL) were used in all of the experiments; 200 μL of the 0.5 M hydride-terminated Si NC solution in toluene was exposed to predetermined amounts of the nitrogen-containing compounds (as tabulated below) and the volume increased to 300 μL using dry toluene (Table 1).

The solution mixture was allowed to react for 3 h. The characteristic orange luminescence of hydride-terminated Si NCs upon exposure to a hand-held UV light was replaced by a faint blue emission. After 3 h, the reaction mixtures were centrifuged at 14 000 rpm for 10 min. The supernatant contained Si NCs that reacted with nitrogen-containing compounds, NH_4Br, or TOAB. TOAB was removed by selective precipitation upon cooling the mixture to *ca.* 0 °C (ice/water bath) and adding 25 μL of acetonitrile as an antisolvent. The solution was centrifuged at 14 000 rpm for 5 min. The supernatant was collected and was found to emit blue light upon exposure to UV illumination.

Direct Synthesis of Dodecyl-Terminated Si NCs (Si NC-B). Na_4Si_4 (0.20g) and NH_4Br (0.40g) were weighed and added to a Schlenk

TABLE 1. Summary of the Titration Procedure Used To Monitor the Influence of Nitrogen-Containing Reagent on Si NC Photoluminescence

hydride-terminated Si NCs in toluene (0.5 M, μL)	nitrogen-containing compound (0.5 M, μL)	volume of toluene added (μL)	total volume (μL)
200	0	100	300
200	10	90	300
200	20	80	300
200	30	70	300
200	40	60	300
200	50	50	300
200	60	40	300
200	70	30	300
200	80	20	300
200	90	10	300
200	100	0	300

flask in a drybox which was then transferred to a Schlenk line. DMF (150 mL) was sparged and added to the starting reagents *via* cannula. The solution was refluxed for 12 h followed by the removal of the solvent *via* a short bridge distillation. Dodecene (40 mL) was sparged, added to the Schlenk flask *via* syringe, and refluxed for 12 h. The liquid was separated from the black/gray solid through centrifugation (8000 rpm for 10 min) and decanted. One quarter of the mixture was placed into a centrifuge tube, and a 3:1 C_2H_5OH/CH_3OH mixture was added. The solution was centrifuged (8000 rpm for 1 h), and a black precipitate was isolated. The precipitate was then dissolved into chloroform and precipitated with CH_3OH. The precipitate was dissolved into toluene and was filtered through a 0.45 μm filter and placed in a vial.

Solution-Phase Reductive Synthesis of Dodecyl Surface-Terminated Si NCs. All reactions were performed under a nitrogen atmosphere. In a typical experiment, 0.0026 mol of $SiCl_4$ (0.3 mL) was dissolved in 1 g of TOAB and 50 mL of anhydrous toluene. The solution was stirred for 20 min, and hydrogen-terminated silicon quantum dots were formed by addition of a stoichiometric amount of hydride reducing agent. Surface-passivated quantum dots were formed by capping the hydrogen-terminated quantum dots with dodecene. After transfer of the solution into a quartz reaction vessel, the passivation was carried out by irradiation with UV light (254 nm) for 4 h.

Surface-passivated quantum dots were purified by size exclusion column chromatography. The solution was filtered of using Millipore 0.45 μm filter paper. The solvent was removed under vacuum, and then the particles were dissolved into 10 mL of methanol. After 5 min sonication, the solution was concentrated down to 1 mL and filtered using a Millipore 0.22 μm syringe filter. The solution was put on the column (φ = 1 cm, 41.0 cm), containing Sephadex gel LH-20 (beads size 25−100 μm) as the stationary phase. Flow rate was set to one drop/4 s, and fractions were collected every 50 drops. Each fraction was checked for luminescence with a hand-held UV lamp (365 nm). Luminescent fractions were collected and concentrated to 1 mL under vacuum. The concentrated solutions contain pure surface-passivated silicon quantum dots.

Characterization. Fourier transform infrared spectroscopy (FT-IR) on the samples H−Si NCs and Si NC-A was performed using a Nicolet Magna 750 IR spectrometer. FT-IR on sample Si NC-C was collected on a Bruker optic GmbH alpha ATR-FT-IR spectrometer. X-ray powder diffraction (XRD) patterns were collected using an INEL XRG 3000 X-ray diffractometer with Cu Kα radiation (λ = 1.54 Å). Thermogravimetric analysis (TGA) was performed on PerkinElmer Pyris 1 using a platinum sample pan and a heating rate of 18 °C/min in air. Proton nuclear magnetic resonance spectra (^{1}H NMR) were collected on 400 MHz Varian Inova instrument. The samples were dissolved in deuterated chloroform ($CDCl_3$).

XPS analyses were performed using a Kratos Axis Ultra instrument operating in energy spectrum mode at 210 W. The base pressure and operating chamber pressure were maintained at 10^{-7} Pa. A monochromatic Al Kα source (λ = 8.34 Å) was used to irradiate the samples, and the spectra were obtained with an electron takeoff angle of 90°. To minimize sample charging, the charge neutralizer filament was used when required. Survey spectra were collected using an elliptical spot with major and minor axis lengths of 2 and 1 mm, respectively, and 160 eV pass energy with a step of 0.33 eV. CasaXPS software (VAMAS) was used to interpret high-resolution (HR) spectra. All of the spectra were internally calibrated to the C 1s emission (284.8 eV). After calibration, the background was subtracted using a Shirley-type background to remove most of the extrinsic loss structure. The full width and half maximum for all of the fitted peaks was maintained below 1.2 eV.

Photoluminescence spectra of the solution-phase samples were acquired using a Varian Cary Eclipse fluorescence spectrometer with a slit width of 5 nm. PL lifetime measurements were performed on samples drop-coated onto silicon wafers coated with 10 drops of the NC suspension (in toluene). Each sample was excited using the 349 nm line of a 25 mW Nd:YLF pulsed laser. Laser pulses (3 kHz) were controlled using a function generator connected to a PL-2001 Q-switched laser driver. Ultrafast lifetime measurements for the blue-emitting Si NCs were performed on a previously described system with temporal resolution of ~200 ps. In brief, the nanoparticles were dissolved in toluene to measure the lifetime decay. The sample was placed in a quartz cuvette and excited with a pulsed FP1060 laser (Fianium US Inc., Eugene, USA) which was frequency quadrupled to excite the samples at λ_{ex} = 355 nm using a fiber optic. The fluorescence decay signal was collected as a function of time as well as wavelength (every 5 nm) by the same fiber optic connected to a nongated multichannel plate detector with an oscilloscope. The laser triggering, the wavelength scanning, and the data acquisition, storage, and processing were controlled using a computer and custom software written in LabVIEW and MATLAB. After each measurement sequence, the laser pulse temporal profile is measured at a wavelength slightly below the excitation laser line.

Transmission electron microscopy (TEM) images of samples H−Si NCs and H−Si NCs treated with allylamine, NH_4Br, and TOAB were obtained using a JEOL-2012 (LaB_6 filament) electron microscope with an accelerating voltage of 200 kV. The TEM images of Si NC-A, Si NC-B, and Si NC-C were obtained on a JEOL 2010 (LaB_6 filament) electron microscope operated at 200 kV. High-resolution TEM images of H−Si NCs treated with NH_4Br and TOAB and Si NC-A were obtained from a Hitachi-9500 electron microscope with an accelerating voltage of 300 kV. HRTEM images of Si NC-B were obtained on a JEOL 2500SE Schottky emitter microscope operating at 200 kV and equipped with a Gatan multiscan camera, and Si NC-C were obtained on a JEOL 2010 (LaB_6 filament) microscope. The TEM samples were prepared by drop-coating freestanding Si NC suspension onto a carbon-coated copper grid with a 400 μm diameter hole. The NC size was averaged over 200 particles, which were calculated using ImageJ software (version 1.45). The HRTEM images were processed using Gatan DigitalMicrograph software (version 2.02.800.0).

Conflict of Interest: The authors declare no competing financial interest.

Acknowledgment. The authors acknowledge funding from the Natural Sciences and Engineering Research Council of Canada (NSERC), Canada Foundation for Innovation (CFI), Alberta Science and Research Investment Program (ASRIP), and University of

Alberta Department of Chemistry. We would like to thank W. C. Moffat and Miranda Skjel for assistance with FT-IR spectroscopy. The staff at the Alberta Centre for Surface Engineering and Sciences (ACSES) is thanked for XPS analysis. H. Qian and K. Cui at National Institute of Nanotechnology (NINT) are thanked for TEM analysis. B. Brown and A. Shukaliak are thanked for assistance with NMR and H−Si NC synthesis, respectively. R. Snitynsky is thanked for useful discussion. The Kauzlarich Group acknowledges funding from DOE (DESC0002289) and NIH (EB008576-01) and thank Prof. L. Marcu for the use of her laser system and Dr. D. Yankelevich for assistance in obtaining the ultrafast lifetime spectra. R.D.T. and A.F. thank the MacDiarmid Institute for funding and MSI for funding through Grant PROP-20106-ICE-MAU.

Supporting Information Available: Characterization of hydride-terminated Si NCs. XPS, FT-IR, lifetime measurements, PL studies, and TEM images of nitrogen-containing Si NCs discussed in this study. This material is available free of charge *via* the Internet at http://pubs.acs.org.

REFERENCES AND NOTES

1. Alivisatos, A. P. Semiconductor Clusters, Nanocrystals, and Quantum Dots. *Science* **1996**, *271*, 933–937.
2. Rogach, A. *Semiconductor Nanocrystal Quantum Dots*; Springer: Berlin, 2008.
3. Michalet, X.; Pinuad, F. F.; Bentolila, L. A.; Tsay, J. M.; Doose, S.; Li, J. J.; Sundaresan, G.; Wu, A. M.; Gambhir, S. S.; Weiss, S. Quantum Dots for Live Cells, *In Vivo* Imaging, and Diagnostics. *Science* **2005**, *307*, 538–544.
4. Biolatti, E.; D'Amico, I.; Zanardi, P.; Rossi, F. Electro-optical Properties of Semiconductor Quantum Dots: Applications to Quantum Information Processing. *Phys. Rev. B* **2002**, *65*, 075306-1–075306-23.
5. Gur, I.; Fromer, N. A.; Geier, M. L.; Alivisatos, A. P. Air-Stable All-Inorganic Nanocrystal Solar Cells Processed from Solution. *Science* **2005**, *310*, 462–465.
6. www.rohs.gov.uk.
7. www.psivida.com
8. Cullis, A. G.; Canham, L. T. Visible Light Emission Due to Quantum Size Effects in Highly Porous Crystalline Silicon. *Nature* **1991**, *353*, 335–338.
9. Sham, T. K.; Jiang, D. T.; Couithard, I.; Lorimer, J. W.; Feng, X. H.; Tan, K. H.; Frigo, S. P.; Rosenberg, R. A.; Houghton, D. C.; Bryskiewicz, B. Origin of Luminescence from Porous Silicon Deduced by Synchrotron-Light-Induced Optical Luminescence. *Nature* **1993**, *363*, 331–334.
10. Cullis, A. G.; Canham, L. T.; Calcott, P. D. J. The Structural and Luminescence Properties of Porous Silicon. *J. Appl. Phys.* **1997**, *82*, 909–965.
11. Polisski, G.; Heckler, H.; Kovalev, D.; Schwartzkopff, M.; Koch, F. Luminescence of Porous Silicon in a Weak Confinement Regime. *Appl. Phys. Lett.* **1998**, *73*, 1107–1109.
12. Li, X.; He, Y.; Talukdar, S. S.; Swihart, M. T. Process for Preparing Macroscopic Qunatities of Brightly Photoluminescent Silicon Nanoparticles with Emission Spanning the Visible Spectrum. *Langmuir* **2003**, *19*, 8490–8496.
13. Pi, X. D.; Liptak, R. W.; Nowak, J. D.; Wells, N. P.; Carter, C. B.; Campbell, S. A.; Kortshagen, U. Air-Stable Full-Visible-Spectrum Emission from Silicon Nanocrystals Synthesized by an All-Gas-Phase Plasma Approach. *Nanotechnology* **2008**, *19*, 245603–245607.
14. Hessel, C. M.; Henderson, E. J.; Veinot, J. G. C. Hydrogen Silsesquioxane: A Molecular Precursor for Nanocrystalline Si-SiO_2 Composites and Freestanding Hydride-Surface-Terminated Silicon Nanoparticles. *Chem. Mater.* **2006**, *18*, 6139–6146.
15. English, D. S.; Pell, L. E.; Yu, Z.; Barbara, P. F.; Korgel, B. A. Size Tunable Visible Luminescence from Individual Organic Monolayer Stabilized Silicon Nanocrystal Quantum Dots. *Nano Lett.* **2002**, *2*, 681–685.
16. Hybertsen, M. S. Absorption and Emission of Light in Nanoscale Silicon Structures. *Phys. Rev. Lett.* **1994**, *72*, 1514–1517.
17. Belyakov, V. A.; Burdov, V. A.; Lockwood, R.; Meldrum, A. Silicon Nanocrystals: Fundamental Theory and Implications for Stimulated Emission. *Adv. Opt. Technol.* **2008**, *2008*, 279502-1–279502-32.
18. Pavesi, L.; Dal Negro, L.; Mazzoleni, L.; Franzo, G.; Priolo, F. Optical Gain in Silicon Nanocrystals. *Nature* **2000**, *408*, 440–444.
19. Khriachtchev, L.; Rasanen, M.; Novikov, S.; Sinkkonen, J. Optical Gain in Si/SiO_2 Lattice: Experimental Evidence with Nanosecond Pulses. *Appl. Phys. Lett.* **2001**, *79*, 1249–1251.
20. Ruan, J.; Fauchet, P. M.; Dal Negro, L.; Cazzanelli, M.; Pavesi, L. Stimulated Emission in Nanocrystalline Silicon Superlattices. *Appl. Phys. Lett.* **2003**, *83*, 5479–5481.
21. Dal Negro, L.; Cazzanelli, M.; Pavesi, L.; Ossicini, S.; Pacifici, D.; Franzo, G.; Priolo, F.; Iacona, F. Dynamics of Stimulated Emission in Silicon Nanocrystals. *Appl. Phys. Lett.* **2003**, *82*, 4636–4639.
22. Wolkin, M. V.; Jorne, J.; Fauchet, P. M.; Allan, G.; Delerue, C. Electronic States and Luminescence in Porous Silicon Quantum Dots: The Role of Oxygen. *Phys. Rev. Lett.* **1999**, *82*, 197–200.
23. Kusova, K.; Cibulka, O.; Dohnalova, K.; Peant, I.; Valenta, J.; Fucikova, A.; Zidek, K.; Lang, J.; Englich, J.; Matejka, P.; *et al.* Brightly Luminescent Organically Capped Silicon Nanocrystals Fabricated at Room Temperature and Atmospheric Prsessure. *ACS Nano* **2010**, *4*, 4495–4504.
24. Belomoin, G.; Therrien, J.; Nayfeh, M. Oxide and Hydrogen Capped Ultrasmall Blue Luminescent Si Nanoparticles. *Appl. Phys. Lett.* **2000**, *77*, 779–781.
25. Valenta, J.; Fucikova, A.; Pelant, I.; Kusova, K.; Dohnalova, K.; Aleknevicius, A.; Cibulka, O.; Fojtik, A.; Kada, G. On the Origin of the Fast Photoluminescence Band in Small Silicon Nanoparticles. *New J. Phys.* **2008**, *10*, 073022-1–073022-6.
26. Svrcek, V.; Sasaki, T.; Shimizu, Y.; Koshizaki, N. Blue Luminescent Silicon Nanocrystals Prepared by ns Pulsed Laser Ablation in Water. *Appl. Phys. Lett.* **2006**, *89*, 213113–213115.
27. Sankaran, R. M.; Holunga, D.; Flagan, R. C.; Giapis, K. P. Synthesis of Blue Luminescent Si Nanoparticles Using Atmospheric-Pressure Microdischarges. *Nano Lett.* **2005**, *5*, 537–541.
28. Holmes, J. D.; Ziegler, K. J.; Doty, R. C.; Pell, L. E.; Johnston, K. P.; Korgel, B. A. Highly Luminescent Silicon Nanocrystals with Discrete Optical Transitions. *J. Am. Chem. Soc.* **2001**, *123*, 3743–3748.
29. Dohnalova, K.; Fucikova, A.; Umesh, C. P.; Humpolickova, J.; Paulusse, J. M. J.; Valenta, J.; Zuilhof, H.; Hof, M.; Gregorkiewicz, T. Microscopic Origin of the Fast Blue-Green Luminescence of Chemically Synthesized Non-oxidized Silicon Quantum Dots. *Small* **2012**, *8*, 3185–3191.
30. Zidek, K.; Pelant, I.; Trojanek, F.; Maly, P.; Gilliot, P.; Honerlage, B.; Oberle, J.; Siller, L.; Little, R.; Horrocks, B. R. Ultrafast Stimulated Emission Due to Quasidirect Transitions in Silicon Nanocrystals. *Phys. Rev. B* **2011**, *84*, 085321-1–085321-9.
31. Dohnalova, K.; Zidek, K.; Ondic, L.; Kusova, K.; Cibulka, O.; Pelant, I. Optical Gain at the F-Band of Oxidized Silicon Nanocrystals. *J. Phys. D: Appl. Phys.* **2009**, *42*, 135102-1–135102-5.
32. Lioudakis, E.; Othonos, A.; Nassiopoulou, A. G. Ultrafast Transient Photoinduced Absorption in Silicon Nanocrystals: Coupling of Oxygen-Related States to Quantized Sublevels. *Appl. Phys. Lett.* **2007**, *90*, 171103-1–171103-3.
33. Luppi, M.; Ossicini, S. *Ab Initio* Study on Oxidized Silicon Clusters and Silicon Nanocrystals Embedded in SiO_2: Beyond the Quantum Confinement Effect. *Phys. Rev. B* **2005**, *71*, 035340-1–035340-15.
34. Brewer, A.; von Haeften, K. *In Situ* Passivation and Blue Luminescence of Silicon Clusters Using a Cluster Beam/H_2O Codeposition Production Method. *Appl. Phys. Lett.* **2009**, *94*, 261102-1–261102-3.
35. Warner, J. H.; Hoshino, A.; Yamamoto, K.; Tilley, R. D. Water Soluble Photoluminescent Silicon Quantum Dots. *Angew. Chem., Int. Ed.* **2005**, *44*, 4550–4554.
36. Shiohara, A.; Hanada, S.; Prabakar, S.; Fujioka, K.; Lim, T. H.; Yamamoto, K.; Northcote, P. T.; Tilley, R. D. Chemical Reactions on Surface Molecules Attached to Silicon Quantum Dots. *J. Am. Chem. Soc.* **2010**, *132*, 248–253.

37. Zou, J.; Baldwin, R. K.; Pettigrew, K. A.; Kauzlarich, S. M. Solution Synthesis of Ultrastable Luminescent Siloxane-Coated Silicon Nanocparticles. *Nano Lett.* **2004**, *4*, 1181–1186.
38. Pettigrew, K. A.; Liu, Q.; Power, P. P.; Kauzlarich, S. M. Solution Synthesis of Alkyl- and Alkyl/Alkoxy-Capped Silicon Nanoparticles *via* Oxidation of Mg_2Si. *Chem. Mater.* **2003**, *15*, 4005–4011.
39. Yang, C. S.; Bley, R. A.; Kauzlarich, S. M.; Lee, H. W. H.; Delgado, G. R. Synthesis of Alkyl-Terminated Silicon Nanoclusters by a Solution Route. *J. Am. Chem. Soc.* **1999**, *121*, 5191–5195.
40. Kelly, J. A.; Shukaliak, A. M.; Fleischauer, M. D.; Veinot, J. G. C. Size-Dependent Reactivity in Hydrosilylation of Silicon Nanocrystals. *J. Am. Chem. Soc.* **2011**, *133*, 9564–9571.
41. Brus, L. E. Electronic Wave Functions in Semiconductor Clusters: Experiment and Theory. *J. Phys. Chem.* **1986**, *90*, 2555–2560.
42. Atkins, T. M.; Thibert, A.; Larsen, D. S.; Dey, S.; Browning, N. D.; Kauzlarich, S. M. Femtosecond Ligand/Core Dynamics of Microwave-Assisted Synthesized Silicon Quantum Dots in Aqueous Solution. *J. Am. Chem. Soc.* **2011**, *133*, 20664–20667.
43. Zhang, X.; Brynda, M.; Britt, R. D.; Carroll, E. C.; Larsen, D. S.; Louie, A. Y.; Kauzlarich, S. M. Synthesis and Characterization of Manganese-Doped Silicon Nanoparticles. *J. Am. Chem. Soc.* **2007**, *129*, 10668–10669.
44. Zhu, H.-L.; Han, F.-D.; Bi, J.-Q.; Bai, Y.-J.; Qi, Y.-X.; Pang, L.-L.; Wang, C.-G.; Li, S.-J. Facile Synthesis of Si_3N_4 Nanocrystals *via* an Organic−Inorganic Reaction Route. *J. Am. Ceram. Soc.* **2009**, *92*, 535–538.
45. Alexander, M. R.; Jones, F. R. The Chemical Environment of Nitrogen in the Surface of Carbon Fibres. *Surf. Interface Anal.* **1994**, *22*, 230–235.
46. Keinan, E. Silicon Hydrides in Organic Synthesis. *Pure Appl. Chem.* **1989**, *61*, 1737–1746.
47. Dasog, M.; Veinot, J. G. C. Solid-State Synthesis of Luminescent Silicon Nitride Nanocrystals. *Chem. Commun.* **2012**, *48*, 3760–3762.
48. Liu, X.; Calata, J. N.; Liang, H.; Shi, W.; Lin, X.; Lin, K.; Qin, G. G. Photoluminescence and Photoluminescence Excitation Mechanisms for Porous Silicon and Silicon Oxynitride. *Mater. Res. Soc. Symp. Proc.* **1999**, *588*, 141–146.
49. Noma, T.; Seol, K. S.; Kato, H.; Fujimaki, M.; Ohki, Y. Origin of Photoluminescence around 2.6−2.9 eV in Silicon Oxynitride. *Appl. Phys. Lett.* **2001**, *79*, 1995–1997.
50. Zhang, L.; Shi, T.; Tang, Z.; Liu, D.; Xi, S.; Li, X.; Lai, W. Carbon-Assisted Growth and High Visible-Light Optical Reflectivity of Amorphous Silicon Oxynitride. *Nanoscale Res. Lett.* **2011**, *6*, 469-1–469-6.
51. Nekrashevich, S. S.; Gritsenko, V. A. Electronic Structure of Silicon Oxynitride: *Ab-Initio* and Experimental Study, Comparison with Silicon Nitride. *J. Appl. Phys.* **2011**, *110*, 114103-1–114103-6.
52. Green, W. H.; Le, K. P.; Grey, J.; Au, T. T.; Sailor, M. J. White Phosphors from a Silicate-Carboxylate Sol−Gel Precursor That Lack Metal Activator Ions. *Science* **1997**, *276*, 1826–1828.
53. Housecroft, C. E.; Sharpe, A. G. *Inorganic Chemistry*; Pearson: Essex, England, 2005.